Well Injectivity Decline for Nonlinear Filtration of Injected Suspension: Semi-Analytical Model

A. S. L. Vaz, Jr.
North Fluminense State University,
Avenida Alberto Lamego 2000,
Campos dos Goytacazes,
28013-602 Rio de Janeiro, Brazil

P. Bedrikovetsky
SPE,
Australian School of Petroleum,
University of Adelaide,
SA 5005, Australia

C. Furtado

A. L.S. de Souza

Petrobras/CENPES

Injectivity decline due to injection of water with particles is a widespread phenomenon in waterflood projects. It happens due to particle capture by rocks and consequent permeability decline and also due to external cake formation on the sandface. Since offshore production environments become ever more complex, particularly in deep water fields, the risk associated with injectivity impairment due to injection of seawater or re-injection of produced water may increase to the point that production by conventional waterflood may cease to be viable. Therefore, it is becoming increasingly important to predict injectivity evolution under such circumstances. The work develops a semi-analytical model for injectivity impairment during a suspension injection for the case of filtration and formation damage coefficients being linear functions of retained particle concentration. The model exhibits limited retained particle accumulation, while the traditional model with a constant filtration coefficient predicts unlimited growth of retained particle concentration. The developed model also predicts the well index stabilization after the decline period. [DOI: 10.1115/1.4002242]

Keywords: injectivity, formation damage, analytical model, well index, deep bed filtration

1 Introduction

Injectivity decline is widely spread during waterflooding. One of the main reasons for the phenomenon is the capture of solid and liquid particles from injected aqueous suspension (seawater, produced water, or any poor quality water) resulting in reduction of permeability and of injection well index [1–4]. The reliable prediction of injectivity index decline is important for the planning and design of well fracturing, acidizing, and other well stimulation techniques. It is also important for the design of water management strategy for waterflood projects.

Injection well behavior prediction under rock clogging due to injection of the colloid/suspension of particles is based on the mathematical modeling of particle transport in porous media [5,6].

The main parameter determining kinetics of particle capture by a porous matrix is the filtration coefficient, which is the ratio between the particle retention rate and the module of the particle flux [6]. The filtration coefficient is a probability for particles to be captured during its transport over the unity distance. Dependency of the filtration coefficient on the retained particle concentration is called the filtration function. Its form highly affects the injectivity decline.

Different forms of filtration function have been presented in the literature [6,7]. The constant filtration coefficient corresponds to low retained concentrations, i.e., to the beginning of the well impairment process. The linear filtration function (the so called blocking function) corresponds to Langmuir particle deposition, where the retention rate is proportional to the number of vacant sites in the porous space and the matrix surface. The blocking filtration function is realized under intermediate retained concentrations [2,8]. Different nonlinear shaped filtration functions have been observed for highly clogged rocks [7,8].

Contributed by the Petroleum Division of ASME for publication in the Journal of Energy Resources technology. Manuscript received January 1, 2009; final manuscript received June 7, 2009; published online xxxxx-xxxxx-xxxxx. Assoc. Editor: Desheng Zhou.

Analytical models for deep bed filtration have been presented for the case of constant filtration and formation damage coefficients for both linear flow geometry (laboratory corefloods) and axisymmetric flow (flow around the vertical well) [6,9,10]. The models exhibit unlimited growth of retained particle accumulation, which is physically unrealistic. Nevertheless, either coreflood or well data show the stabilized permeability with time. The analytical model for coreflood with blocking filtration function also exhibits the stabilized injectivity index [6,11,12].

In the current work, a semi-analytical model for axisymmetric flow around the vertical well is developed for a blocking filtration function. The particle capture stops after reaching the maximum (critical) value by the retained concentration in each point of the drainage volume. The injectivity index stabilizes when the retained concentration grows up to the critical value in a well neighborhood.

The structure of the paper is as follows. First, we describe the mathematical model for suspension filtration and rock clogging under Langmuir particle retention. Then, we discuss a semi-analytical model for axisymmetric flow with detailed derivations. Afterward, the results of impedance prediction with a sensitivity analysis are presented.

2 Mathematical Model for Deep Bed Filtration

During seawater injection, mainly solid particles penetrate into the reservoir; their retention in rock results in permeability decline and a consequent decrease in well injectivity index. Oily water injection during produced water re-injection (PWRI) also results in injectivity impairment.

Deep bed filtration with similar modeling challenges occurs during drilling fluid invasion into formation with consequent permeability damage [13–15]. It also occurs during produced water disposal in aquifers [16,17].

It is assumed that all injected particles have the same filtration properties, allowing us to introduce the overall suspended and retained particle concentrations. Figure 1 shows the suspension

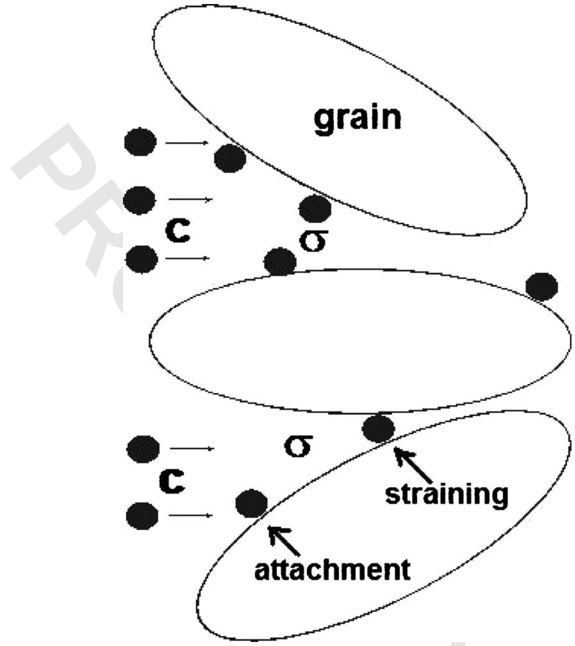

Fig. 1 Suspended and retained particle concentrations in porous space

concentration c of moving particles and the concentration σ of particles attached to grain surfaces and captured in thin throats by size exclusion.

Following Refs. [4,6,18,19], let us describe the mathematical model for flow of suspensions in porous media in the axisymmetric geometry of vertical wells.

The conservation of suspended and retained particles in porous media is

$$\phi\frac{\partial c}{\partial t} + \frac{q}{2\pi rh}\frac{\partial c}{\partial r} = -\frac{\partial \sigma}{\partial t} \tag{1}$$

It is assumed that water is incompressible, and particle retention by rock does not change the total volume of the system "water particles." It results in the conservation of the flux q.

Classical filtration theory assumes that the retention rate is proportional to the particle advective flux cU, i.e., increase in either suspended concentration or velocity in number of times results in the same number of times increase in the number of particles, which are transported to vacancies in rocks per unit of time. The proportionality coefficient λ depends on σ and is called the filtration function $\lambda(\sigma)$,

$$\frac{\partial \sigma}{\partial t} = \lambda(\sigma)c\frac{q}{2\pi rh} \tag{2}$$

We assume that the capture rate is also proportional to the number of vacancies (Langmuir's hypothesis). If A is a specific rock surface and b is an "individual" area on the grain surface engaged by one retained particle, the vacancy concentration is proportional to the free vacant surface, which equals $A-b\sigma$ (Fig. 1).

Finally, the retention rate is proportional to

$$(A-b\sigma)cU$$

Introducing the proportionality coefficient yields the kinetic equation for retention rate,

$$\frac{\partial \sigma}{\partial t} = \lambda_0\left(1-\frac{\sigma}{\sigma_m}\right)c\frac{q}{2\pi rh} \tag{3}$$

The comparison between Eqs. (2) and (3) shows that the filtration function in Eq. (3) is linear with respect to retention concentration,

$$\lambda(\sigma) = \begin{cases} \lambda_0\left(1-\dfrac{\sigma}{\sigma_m}\right), & \sigma < \sigma_m \\ 0, & \sigma > \sigma_m \end{cases}$$

If linear dependency in Eq. (3) for $\lambda(\sigma)$ holds for the whole interval of retention concentration variation, the maximum of retention concentration σ_m corresponds to the case where the overall vacant grain surface is filled by particles; i.e., σ_m is proportional to the initial number of vacancies. If $\lambda(\sigma)$ is linear just for some initial interval of σ and becomes nonlinear for larger values of retained concentration, σ_m is just a coefficient in the equation for a straight line without any specific physics meaning.

So, the retention rate is characterized by two constants—by the initial filtration coefficient λ_0 and by the maximum retention concentration σ_m. Parameters λ_0 and σ_m depend on the salinity and pH of the injected water, on the mineral composition of grains, on particle size, on its wettability, on temperature, etc.; i.e., two constants are determined by the rock and the injected fluid.

If the retention concentration is negligibly smaller than the initial concentration of vacancies, the retained particles do not affect the vacancy concentration and do not change the retention conditions, and the filtration function is constant. Formally, it corresponds to an infinite value of the maximum retention concentration σ_m.

So called collective effects of particle interaction at high concentrations lead to the nonlinear filtration coefficient $\lambda=\lambda(\sigma)$. Its form depends on brine salinity, pH, electric DLVO forces, etc. [20–22]. AQ: #2

Particle retention results in permeability decrease; i.e., permeability is σ dependent:

$$\frac{q}{2\pi rh} = -\frac{k_0 k(\sigma)}{\mu}\frac{\partial p}{\partial r}, \qquad k(\sigma) = \frac{1}{1+\beta\sigma(1+\beta_2\sigma/\beta)} \tag{4}$$

Different empirical formulas for permeability decrease with an increase in retained concentration have been proposed in the literature [14,22–26]. Usually, a linear function of σ in the denominator of Eq. (4) with $\beta_2=0$ is used in the expression for formation damage function $k(\sigma)$, where β is called the formation damage coefficient [9,10].

A more general form of the denominator in Eq. (4) with nonzero β_2 is used in Ref. [24] to adjust coreflood injectivity impairment data. The case of Eq. (4) corresponds to the linear function of formation damage coefficient β versus retention concentration σ, which corresponds to a quadratic polynomial for reciprocal to formation damage function $k(\sigma)$. Further in the text, β_2 is called the second formation damage coefficient.

The coefficients β and β_2 are empirical constants characterizing formation damage; they depend on the rock and the injected suspension properties.

Systems (1) and (2) consist of two equations for two unknowns—c and σ. For the injection of constant concentration suspension into a clean bed, systems (1) and (3) are subject to the following initial and boundary conditions:

$$t=0: c=\sigma=0, \quad r=r_w: c=c^0 \tag{5}$$

The boundary condition (5) is set at the wellbore $r=r_w$ (Fig. 2).

Introduce dimensionless coordinate and time

$$X=\frac{r^2}{R_c^2}, \quad t_D=\frac{qt}{\pi\phi h R_c^2} \tag{6}$$

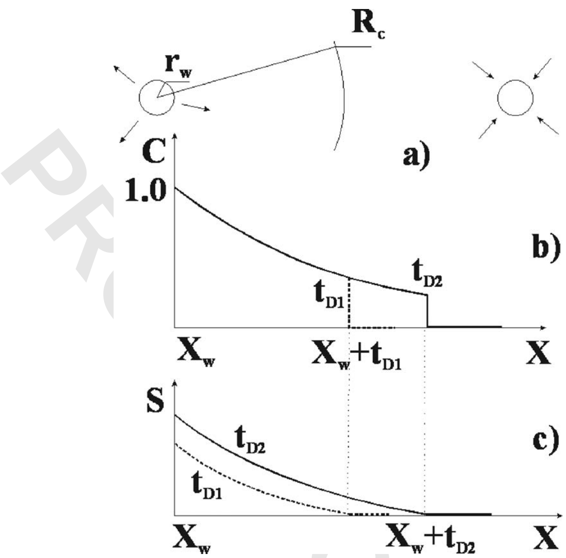

Fig. 2 Schematic for injected suspension propagation between injection and production well: (*a*) contour radius is equal to half-distance between injector and producer; (*b*) profile of suspension concentration is steady state behind the concentration front; (*c*) gradual accumulation of retained particles behind the concentration front

The dimensionless time with the pore volumes injected (p.v.i.) unit is identical to that in waterflooding, while the linear coordinate X is equal to the square of the dimensionless radius [26]. The drainage radius is equal to the half-distance between injection and production wells (Fig. 2).

Substitution of Eq. (6) along with dimensionless concentrations, pressure, and filtration function

$$C = \frac{c}{c^0}, \quad S = \frac{\sigma}{\phi c^0}, \quad p_D = \frac{4\pi h k_0 p}{q\mu}, \quad \Lambda(S) = \lambda(\sigma) R_c \tag{7}$$

into systems (1), (2), and (4) yields

$$\frac{\partial C}{\partial t_D} + \frac{\partial C}{\partial X} = -\frac{\partial S}{\partial t_D} \tag{8}$$

$$\frac{\partial S}{\partial t_D} = \frac{\Lambda(S)}{2\sqrt{X}} C \tag{9}$$

$$1 = -\frac{X}{(1 + \beta\phi c^0 S + \beta_2(\phi c^0)^2 S^2)} \frac{\partial p_D}{\partial X} \tag{10}$$

Initial and boundary conditions (5) for dimensionless variables (Eqs. (6) and (7)) take the form

$$t_D = 0{:}\, C = S = 0 \ \text{ and } \ X = X_W = (r_W/R_c)^2{:}\, C = 1 \tag{11}$$

Several analytical solutions of the problem (Eqs. (1), (2), and (5)) have been reported in the literature [6]. A semi-analytical solution for the clean bed injection problem (Eq. (5)), for the case of filtration and formation damage coefficients linear with respect to retention concentration, is presented in the next section.

While the initial-boundary problem (Eqs. (1), (2), and (11)) is solved, pressure distribution along linear coordinate X during flooding can be found from Eq. (4) by a direct integration of the pressure gradient in X from the well radius X_w to the contour radius $X_c = 1$.

3 Semi-Analytical Model for Axisymmetric Deep Bed Filtration

Let us derive a semi-analytical solution for the axisymmetric (radial) problem of deep bed filtration for any arbitrary filtration function $\lambda(\sigma)$.

Introduce potential

$$\Phi(S) = \int_0^S \frac{ds}{\Lambda(s)} \tag{12}$$

From Eq. (9), it follows that

$$C = \frac{\partial[2\sqrt{X}\Phi(S)]}{\partial t_D} \tag{13}$$

Substituting Eq. (13) in Eq. (8) yields

$$\frac{\partial}{\partial t_D}\left\{\frac{\partial}{\partial t_D}[2\sqrt{X}\Phi(S)]\right\} + \frac{\partial}{\partial X}\left\{\frac{\partial}{\partial t_D}[2\sqrt{X}\Phi(S)]\right\} = -\frac{\partial S}{\partial t_D} \tag{14}$$

Changing the order of differentiation in the second term of Eq. (14) results in

$$\frac{\partial}{\partial t_D}\left\{\frac{\partial}{\partial t_D}[2\sqrt{X}\Phi(S)] + \frac{\partial}{\partial X}[2\sqrt{X}\Phi(S)] + S\right\} = 0 \tag{15}$$

The integration of Eq. (15) in t_D accounting for initial conditions (11) yields

$$\frac{\partial}{\partial t_D}[2\sqrt{X}\Phi(S)] + \frac{\partial}{\partial X}[2\sqrt{X}\Phi(S)] + S = \left\{\frac{\partial}{\partial t_D}[2\sqrt{X}\Phi(S)] + \frac{\partial}{\partial X}[2\sqrt{X}\Phi(S)] + S\right\}_{t_D=0} \tag{16}$$

As it follows from initial conditions (11), the right hand side of Eq. (16) is equal to zero; i.e., Eq. (16) becomes

$$\frac{\partial}{\partial t_D}[2\sqrt{X}\Phi(S)] + \frac{\partial}{\partial X}[2\sqrt{X}\Phi(S)] + S = 0 \tag{17}$$

So, the introduction of potential (12) results in decreasing of the order of the partial differential equation of mass balance (8) by 1.

Performing differentiation in Eq. (17) accounting for Eq. (12) results in

$$\frac{\partial S}{\partial t_D} + \frac{\partial S}{\partial X} = \left(-\frac{\Phi(S)}{\sqrt{X}} - S\right)\frac{\Lambda(S)}{2\sqrt{X}} \tag{18}$$

The obtained first order hyperbolic Eq. (18) can be solved by method of characteristics.

Let us express first order partial differential Eq. (18) in characteristic form,

$$\frac{\partial t_D}{\partial X} = 1 \tag{19}$$

$$\frac{dS}{dX} = \left(-\frac{\Phi(S)}{\sqrt{X}} - S\right)\frac{\Lambda(S)}{2\sqrt{X}} \tag{20}$$

From the boundary condition on the well (Eq. (11)), it follows that for any moment t'_D

$$2\sqrt{X_w}\Phi(S) = t'_D \tag{21}$$

allowing expression of retained saturation on the wellbore

$$S(X_w, t'_D) = \Phi^{-1}\left(\frac{t'_D}{2\sqrt{X_w}}\right) \tag{22}$$

Here, Φ^{-1} is an inverse function to $\Phi(S)$ (see Eq. (12)).

As it follows from Eq. (19), the characteristic line crossing any arbitrary point (X, t_D) also crosses point (X_w, t'_D) (see also Fig. 3),

PROOF COPY [JERT-09-1001] 013003JRG

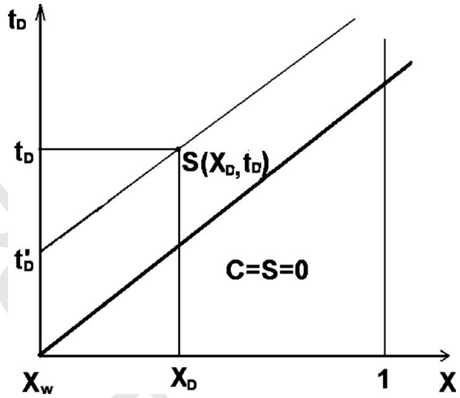

Fig. 3 Concentration front and characteristic line on the plane (X, t_D)

$$t'_D = t_D - X + X_w \tag{23}$$

It results in the Cauchy condition for the ordinary differential Eq. (20),

$$X = X_w : S = \Phi^{-1}\left(\frac{t_D - X + X_w}{2\sqrt{X_w}}\right) \tag{24}$$

Ordinary differential Eq. (20) subject to Cauchy condition (24) can be solved numerically.

Ahead of the concentration front $X > X_f = t_D - X_w$, suspended and retained concentrations are equal to zero. The retained concentration is continuous along the front, $S=0$, while the suspension concentration suffers discontinuity. Substituting Eq. (9) into Eq. (8) and accounting for zero retained concentration on the suspended concentration shock, we obtain

$$\frac{\partial C}{\partial t_D} + \frac{\partial C}{\partial X} = -\frac{\Lambda(0)}{2\sqrt{X}}C \tag{25}$$

Front $X = X_w + t_D$ is a characteristic line, which allows us to calculate suspended concentration behind the front from Eq. (25),

$$C(X_f(t_D), t_D) = \exp[-\Lambda(0)(\sqrt{X_f} - \sqrt{X_w})] = \exp[-\Lambda(0)(\sqrt{X_w + t_D} - \sqrt{X_w})] \tag{26}$$

Consider the particular case of linear filtration coefficient:

$$\Lambda(S) = \lambda_0 R_c\left(1 - \frac{S}{S_m}\right) \tag{27}$$

The potential (12) is

$$\Phi(S) = -\frac{S_m}{\lambda_0 R_c}\ln\left(1 - \frac{S}{S_m}\right) \tag{28}$$

Equation (20) and the Cauchy condition become

$$\frac{dS}{dX} = \left(\frac{S_m}{\lambda_0 R_c \sqrt{X}}\ln\left(1 - \frac{S}{S_m}\right) - S\right)\frac{\lambda_0 R_c}{2\sqrt{X}}\left(1 - \frac{S}{S_m}\right) \tag{29}$$

$$X = X_w : S = S_m\left[1 - \exp\left(-\frac{\lambda_0 R_c}{S_m}\frac{t_D - X + X_w}{2\sqrt{X_w}}\right)\right] \tag{30}$$

The structure of the suspension flow zone is shown in Fig. 3. Suspended and retained concentrations are equal to zero ahead of the front, which moves with carrier water velocity. Suspended concentration jumps from zero to the value of $c^-(r_f, t)$ on the front. The suspended concentration behind the front is found from the condition on the characteristic line with $\sigma=0$, which coincides with the concentration front [26]:

$$c^-(r_f(t), t) = c^0 \exp\left[-\lambda(0)\left(\sqrt{r_w^2 + \frac{qt}{\pi\phi h}} - r_w\right)\right] \tag{31}$$

The retained concentration behind the front is given by the solution of the first order ordinary differential Eq. (20). For the case of the linear filtration function (Eq. (27)), the solution is given by formula (29).

The solution $S(X, t_D)$ of the problem (Eqs. (29) and (30)) in the behind-the-front region is obtained by the Runge–Kutta method. The suspended concentration $c(r,t)$ is obtained by Eq. (9) using the retained concentration $s(r,t)$.

Figure 4 presents profiles of suspended and retained concentrations, (a) and (b), respectively, at five different moments. The values of injectivity damage coefficients and other parameters are obtained in Ref. [12] by the treatment of coreflood data [27]: $\lambda_0 = 10\ \text{m}^{-1}$, $\beta=100$, $\beta_2=-1000$, $\sigma_m=0.025$, $c_0=10$ ppm, $R_c=500$ m, $r_w=0.1$ m, and $h=30$ m. The axes X for the profiles extend from well $X=X_w$ until the value that corresponds to $r=0.5$ m.

The suspended concentration gradually increases with time in each reservoir point for the calculated case of linear filtration coefficient. This behavior is typical of the declining filtration coefficient—the outlet concentration after the breakthrough remains constant for a constant filtration coefficient. Gradual accumulation of retained concentration with time is shown in Fig. 4(*b*).

The dimensionless pressure drop between injector and reservoir (drawdown) is

$$J = \frac{\Delta P}{\Delta P_0} = -\frac{1}{\ln(X_w)}\int_{X_w}^{1} -\frac{\partial p_D}{\partial X}dX \tag{32}$$

Let us express pressure gradient via deposited concentration from Eq. (10) and substitute it into Eq. (32),

$$J(t_D) = 1 - \frac{\beta\phi c^0}{\ln(X_w)}\int_{X_w}^{1}\frac{S(X,t_D)}{X}dX - \frac{\beta_2(\phi c^0)^2}{\ln(X_w)}\int_{X_w}^{1}\frac{S^2(X,t_D)}{X}dX \tag{33}$$

The well impedance (Eq. (33)) is obtained by numerical integration in X of expressions containing retained concentration distribution $S(X, t_D)$, as calculated from Eqs. (29) and (30).

4 Calculations of Well Injectivity Index

Let us show how to use formula (33) and the values of four injectivity damage parameters λ_0, σ_m, β, and β_2, as obtained by the treatment of coreflood data [12], for well injectivity decline prediction.

The model for vertical well injectivity decline consists of nonlinear deep bed filtration equations for axisymmetric flow geometry; see Eqs. (1), (3), and (4). An exact semi-analytical solution of the radial deep bed filtration problem (Eqs. (29) and (30)) allows us to calculate well impedance versus time (Eq. (33)).

Figure 5 shows the sensitivity of the impedance curve with respect to the second formation damage coefficient, while the filtration coefficient is constant; i.e., σ_m tends to infinity. A 1 month injection period in Fig. 5(*a*) corresponds to 6×10^{-3} p.v.i. in Fig. 5(*b*). The default case corresponds to linear filtration with constant filtration and formation damage coefficients, $\lambda_0=10\ \text{m}^{-1}$, $\beta=50$, and $\beta_2=0$. Curves 2 and 3 correspond to values of the second formation damage coefficient $\beta_2=200$ and $\beta_2=-200$, respectively. The β_2-values are in the range of those obtained from coreflood data [27].

If compared with the default case with $\beta_2=0$, adding the quadratic term $\beta_2\sigma^2$ with the positive β_2 coefficient results in impedance increase (curve 2). Introduction of the quadratic term $\beta_2\sigma^2$ with the negative β_2 coefficient results in impedance decrease (curve 3). The impedance curve is concave for the case of the positive second formation damage coefficient and is convex for negative β_2. The significant difference between the impedance

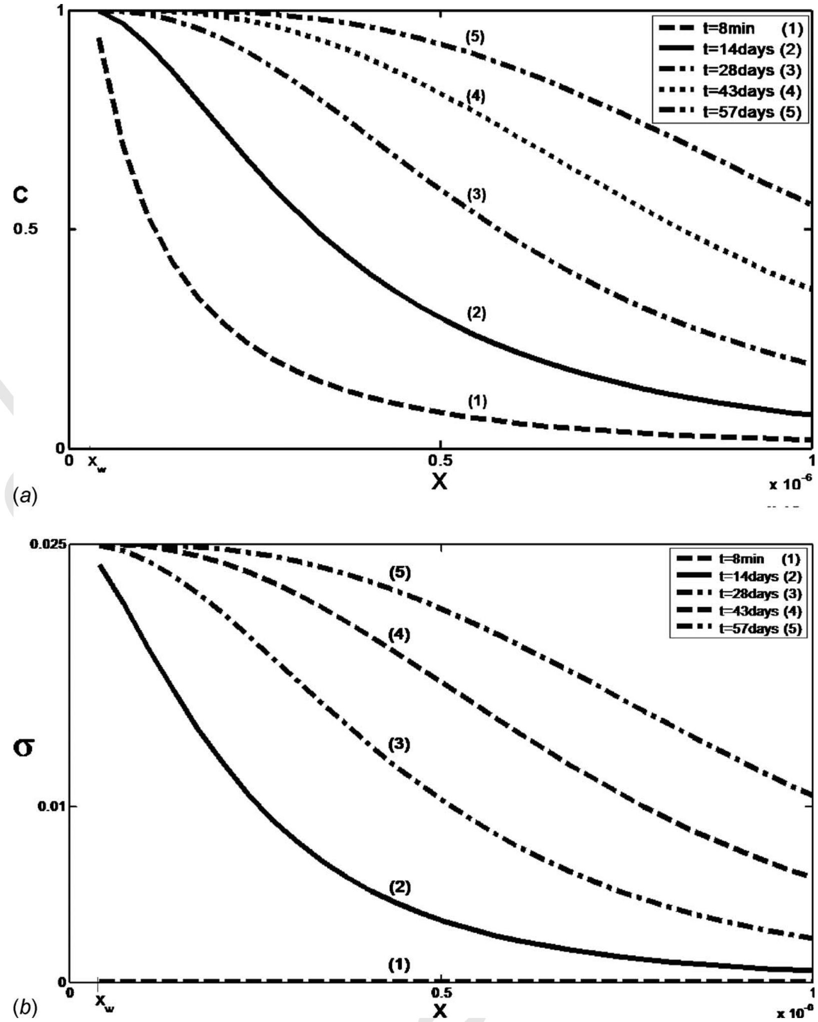

Fig. 4 Dynamics of (*a*) suspended and (*b*) retained concentration profiles during suspension injection in vertical well

curves with zero, positive, and negative β_2 starts to appear after 2×10^{-3} p.v.i. (10 days). The curves almost coincide before the injection of 10^{-3} p.v.

After 1 month of injection, the injectivity index decreases 2.4 times for the constant formation damage coefficient ($\beta_2=0$). It decreases 2.65 times for $\beta_2=200$ and 2.15 times for $\beta_2=-200$.

Let us discuss the effect of the nonconstant filtration coefficient on impedance growth. Figure 6 presents impedance curves for constant formation damage coefficients $\beta=50$ and $\beta_2=0$. The initial filtration coefficient $\lambda_0=10\ \mathrm{m}^{-1}$. Curves 1–5 correspond to the following values for maximum retained concentration: infinity, 0.1, 0.05, 0.025, and 0.0015, respectively. So, the filtration function decreases in order of the curve number increase. The larger the filtration function, the higher the retained particle concentration and the higher the impedance. Therefore, curves 1–5 follow in the order of the impedance decrease.

Curve 1 is linear due to the constant filtration coefficient. Impedance curves 2–5 stabilize with time; i.e., its time derivative tends to zero when time tends to infinity. It is explained by reaching the maximum retention concentration σ_m in each point around the well. The higher the distance to the point from the injector, the later the maximum retention concentration will be reached. Therefore, curves 2–5 follow in order of decrease in the stabilization time. The moments of impedance stabilization are 200 days, 106 days, 50 days, and 3 days, for curves 2–5, respectively.

Since the impedance function asymptotically reaches maximum for retained concentration that is equal to the critical value σ_m, from Eq. (33) follows formula for the maximum impedance,

$$J(t\rightarrow\infty)=1+\beta\sigma_m+\beta_2\sigma_m^2 \qquad (34)$$

After the long-term injection, the injectivity index decreases 6.0, 3.5, 2.3, and 1.1 times for curves 2–5, respectively.

In offshore waterflood operations, the injectivity index stabilization at some reduced value happens quite often [3,9,19]. The usual explanation is well fracturing, where the fracture opens due to high pressure near the injector because of reduced permeability; it propagates into the formation during further permeability decline and increase in hydraulic resistivity for leak-off. Another explanation is erosion of external and internal filter cakes, where the pressure gradient, increased due to permeability decline, drags particles from cakes in situ porous media and on the inner well surface.

Reaching the maximum retention concentration, where particle capture by the rock does not happen anymore, is another explanation of well injectivity index stabilization.

Let us compare the impedance growth curves for constant and for linear filtration and formation damage functions. Straight line 1 in Fig. 7 corresponds to constant filtration and formation damage coefficients: $\lambda_0=10\ \mathrm{m}^{-1}$ and $\beta=50$. For curves 2–6, values of λ_0 and β are the same as that for case 1.

The second formation damage coefficient for curve 2 is equal to 1000. For small retention concentrations at the beginning of in-

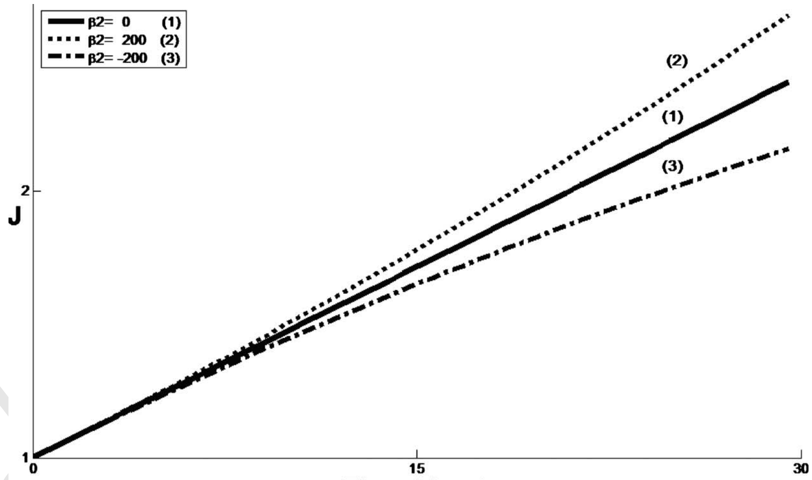

(*a*)

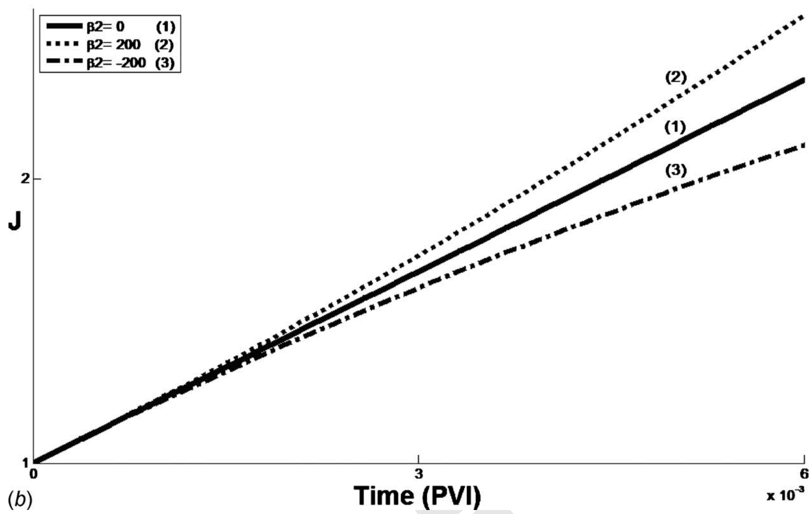

(*b*)

Fig. 5 Effect of two formation damage coefficients β and β_2 on well impedance curve: (*a*) impedance versus real time; (*b*) impedance versus p.v.i.

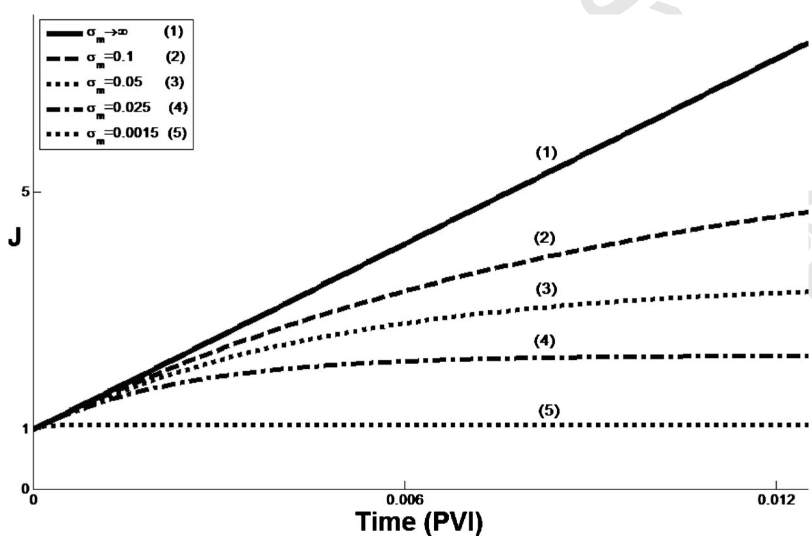

Fig. 6 Sensitivity of impedance curve to variation in filtration function: impedance versus p.v.i.

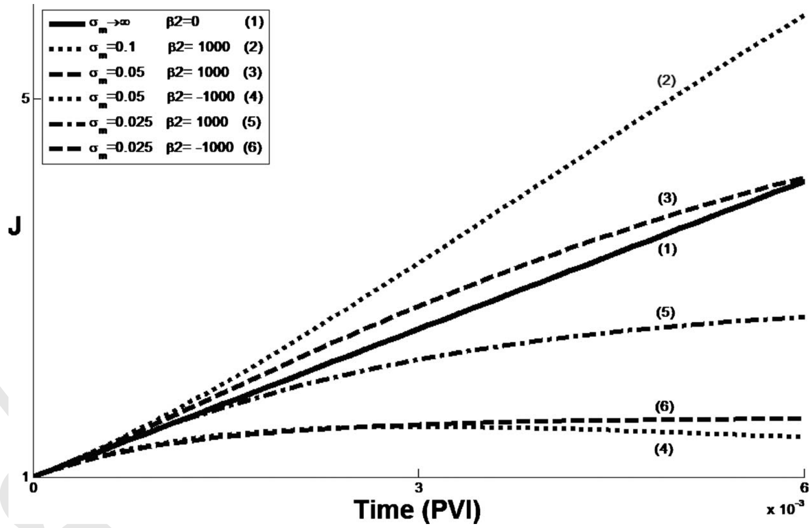

Fig. 7 Monotonic and nonmonotonic impedance curves

jection, the values of filtration functions for cases 1 and 2 are almost equal. Due to the high value of the second formation damage coefficient for curve 2, it is located above the straight line 1 for small times. Curve 2 stabilizes with time, while the straight line 1 grows unlimitedly. Therefore, at some moment, curve 2 intersects line 1 and tends to a constant value at large times.

Curve 3 has a lower maximum retention concentration value if compared with curve 2. Therefore, curve 3 is located above line 1 and below curve 2 at small times. Curve 3 crosses line 1 and stabilize faster than curve 2.

The value of maximum retention concentration for curve 5 is lower than that for curve 3. Curve 5 is located above line 1 and below the curve 3 at small times. Curve 5 crosses line 1 and stabilize faster than curve 3.

Curves 2, 3, and 5 exhibit a monotonic growth. For positive σ-values and positive second formation damage coefficient, the derivative of reciprocal to formation damage function $k(\sigma)$ (see Eq. (4))

$$(\beta_2\sigma^2 + \beta\sigma + 1)' = 2\beta_2\sigma + \beta > 0$$

is always positive; i.e., the hydraulic resistance of retained particles increases during the deposition.

Curves 4 and 6 correspond to the negative second formation damage coefficient $\beta_2 = -1000$. The derivative of the formation damage function $2\beta_2\sigma + \beta$ is positive for low σ-values, i.e., for $\sigma < -\beta/2\beta_2$ (Fig. 8). For higher retention concentration values, $\sigma > -\beta/2\beta_2$, the derivative is negative; accumulation of retained particles results in the reduction of hydraulic resistivity. This effect is physically unrealistic.

In case 4, $\sigma_m = 0.05$, $\beta_2 = -1000$, and $\beta = 50$; so, $-\beta/2\beta_2 = 0.025$, which is less than σ_m; i.e., the hydraulic resistivity increases for retention concentration varying from zero to 0.025 and decreases afterward for retention concentration varying from 0.025 to 0.05. Curve 4 decreases for $\sigma > 0.025$. This behavior is unrealistic. The paradox is caused by approximation of the formation damage function by the quadratic polynomial based on J-values for small retention concentrations (Fig. 8). If the dependency $\lambda = \lambda(\sigma)$ has a negative second derivative, its approximation by the linear function (3) causes the high value for the maximum retained concentration (Fig. 9), resulting in inequality $\sigma_m > -\beta/2\beta_2$. In this case, the model with linear filtration coefficient (3) is not valid.

For case 6, $\sigma_m = 0.025$ and $-\beta/2\beta_2 = 0.025 = \sigma_m$. During an increase in retention concentration from zero to σ_m, where σ tends to σ_m asymptotically, the hydraulic resistivity increases, which is shown by the behavior of curve 6.

Figure 10 presents injectivity index decline for the cases discussed in Fig. 7. The declined form of injectivity index versus time does allow distinguishing linear and nonlinear well behavior, while the impedance plot clearly shows a linear well behavior for the case of constant injectivity damage coefficients and nonlinear

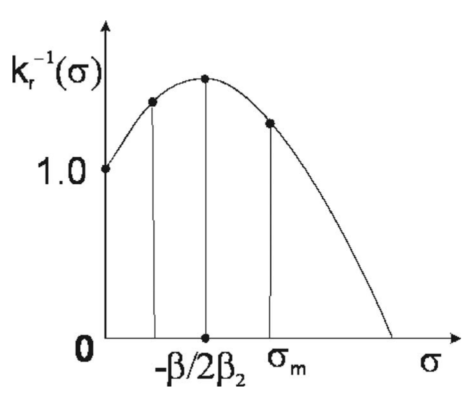

Fig. 8 Nonmonotonic behavior of reciprocal to formation damage function due to linear interpolation of formation damage coefficient

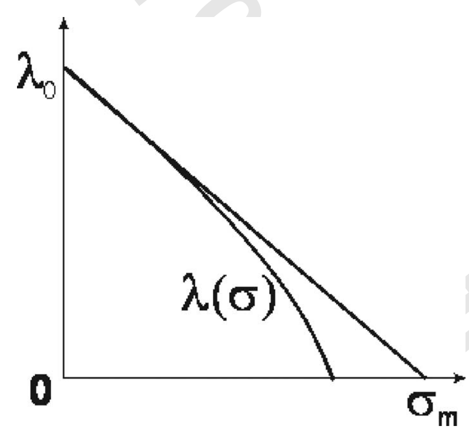

Fig. 9 Overestimated value of maximum retained concentration due to linear approximation of the filtration function

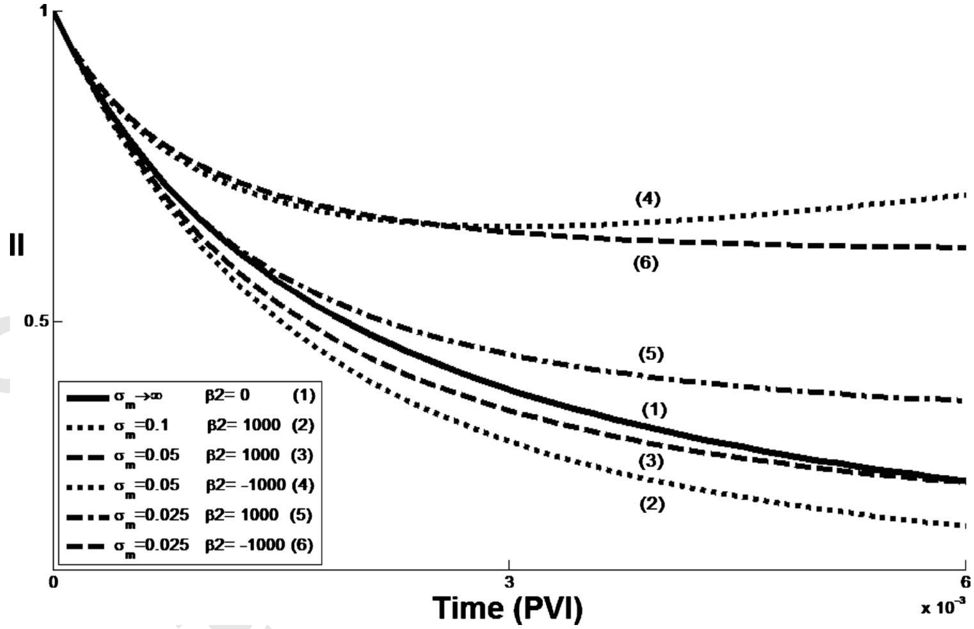

Fig. 10 Injectivity decline analysis using well index curves

curves for varying λ and β. It shows the advantage to analyze injectivity impairment in coordinates "impedance versus time."

The proposed three-point-pressure method [12] can be implemented into a simple, robust, and compact tool for applications in on-site field conditions. Figure 11 shows the use of the tool at the sea platform. Direct measurements data of the rate and of pressures in three core points are treated by the computer program with optimization algorithm minimizing the deviation between the modeling and coreflood data. It allows us to determine the four injectivity damage coefficients λ_0, σ_m, β, and β_2 from coreflood data. Then, the impedance and well index are recalculated for the axisymmetric flow of a vertical well (Eq. (33)) and also for flow geometries of horizontal, fractured, and perforated wells using the analytical solutions for 3D flow problems [28].

5 Conclusions

Injectivity decline due to rock clogging by the injected suspension with linear filtration and formation damage functions allows for semi-analytical modeling.

The impedance for injectivity damage parameters that are linear functions of the retained concentration monotonically increases and asymptotically tends to a limit constant, while the impedance for constant injectivity damage parameters linearly grows with time.

The injectivity index stabilizes after the retained particle concentration reaches its maximum value in some neighborhood of the injector.

Fig. 11 Using the three-point-pressure tool at sea platform

The well behavior for constant injectivity damage parameters can be distinguished from that for linear function parameters by increasing impedance curves, not by declining well index curves.

Acknowledgment

The authors thank Petrobras for generous sponsorship of the research project during many years and Dr. Farid Shecaira and Eng. Alexandre Guedes Siqueira (Petrobras/CENPES) for fruitful support and encouragement. Many thanks are due to Prof. P. Currie (Delft University of Technology), Prof. Yannis Yortsos (University of Southern California), and Prof. A. Shapiro for fruitful discussions.

Nomenclature

Latin Letters

A = specific rock surface, $[L]^2$
b = area on grain surface filled by one retained particle, $[L]^2$
c = suspension particle concentration
c^o = injected suspension concentration
h = formation thickness, $[L]$
II = injectivity index
J = impedance
k = permeability, $[L]^2$
L = core length, $[L]$
p = pressure, $[M][T]^{-2}[L]^{-1}$
r = radius, $[L]$
R_c = drainage (contour) radius, $[L]$
q = injection rate, $[L^3/T]$
t = time, $[T]$
U = Darcy velocity, $[L][T]^{-1}$
x = coordinate in linear geometry, $[L]$
X = dimensionless coordinate in radial geometry

Greek Letters

β = formation damage coefficient
β_2 = formation damage coefficient
λ = filtration coefficient $[L]^{-1}$
λ_0 = value of filtration coefficient for σ=0, $[L]^{-1}$

μ = viscosity of water, $[M][T]^{-1}[L]^{-1}$
σ = deposited particle concentration
Φ = porosity
Φ = potential

Superscripts/Subscripts

0 = initial
f = front
m = maximum
D = dimensionless
w = well

References

[1] Civan, F., 2006, *Reservoir Formation Damage (Fundamentals, Modeling, Assessment, and Mitigation)*, 2nd ed., Gulf, Houston, TX, p. 742.

[2] Wojtanowicz, A. K., Krilov, Z., and Langlinais, J. P., 1987, "Study on the Effect of Pore Blocking Mechanisms on Formation Damage," Production Operations Symposium, Oklahoma City, OK, Mar. 8–10, Paper No. SPE 16233.

[3] Barkman, J. H., and Davidson, D. H., 1972, "Measuring Water Quality and Predicting Well Impairment," JPT, **24**(7), pp. 865–873.

[4] Sharma, M. M., and Yortsos, Y. C., 1987, "Transport of Particulate Suspensions in Porous Media: Model Formulation," AIChE J., **33**(10), pp. 1636–1643.

[5] Civan, F., 2007, "Formation Damage Mechanisms and Their Phenomenological Modeling—An Overview," European Formation Damage Conference, Sheveningen, The Netherlands, May 30–Jun. 1, Paper No. SPE-107857.

[6] Herzig, J. P., Leclerc, D. M., and le Goff, P., 1970, "Flow of Suspensions Through Porous Media—Application to Deep Filtration," Ind. Eng. Chem., **62**(5), pp. 8–35.

[7] Alvarez, A. C., Bedrikovetsky, P., Hime, G., Marchesin, D., and Rodríguez, J. R., 2006, "A Fast Inverse Solver for the Filtration Function for Flow of Water With Particles in Porous Media," Inverse Probl., **22**, pp. 69–88.

[8] Kuhnen, F., Barmettler, K., Bhattacharjee, S., Elimelech, M., and Kretzschmar, R., 2000, "Transport of Iron Oxide Colloids in Packed Quartz Sand Media: Monolayer and Multilayer Deposition," J. Colloid Interface Sci., **231**, pp. 32–41.

[9] Pang, S., and Sharma, M. M., 1997, "A Model for Predicting Injectivity Decline in Water-Injection Wells," Paper No. SPEFE-28489, pp. 194–201.

[10] Bedrikovetsky, P., da Silva, M. J., da Silva, M. F., Siqueira, A. G., de Souza, A. L. S., and Furtado, C., 2005, "Well-History-Based Prediction of Injectivity Decline During Seawater Flooding," SPE Sixth European Formation Damage Conference, Scheveningen, The Netherlands, May 25–27, Paper No. SPE-93886.

[11] Soo, H., and Radke, C. J., 1986, "A Filtration Model for the Flow of Dilute, Stable Emulsions in Porous Media—I Theory," Chem. Eng. Sci., **41**(2), pp. 263–272.

[12] Bedrikovetsky, P., Vaz, A. S. L., Jr., Furtado, C. A., and de Souza, A. L. S., 2008, "Formation Damage Evaluation From Non-Linear Skin Growth During Coreflooding," SPE International Symposium and Exhibition on Formation Damage Control, Lafayette, LA, Feb. 13–15, Paper No. SPE-112509.

[13] Bailey, L., Boek, E. S., Jacques, S. D. M., Boassen, T., Selle, O. M., Argillier, J.-F., and Longeron, D. G., 2000, "Particulate Invasion From Drilling Fluids," SPE J., **5**(4), pp. 412–419.

[14] Suryanarayana, P. V., Wu, Z., Ramalho, J., and Himes, R., 2007, "Dynamic Modelling of Invasion Damage and Impact on Production in Horizontal Wells," SPE Reservoir Eval. Eng., **10**(4), pp. 348–358.

[15] Tang, Y., Yildiz, T., Ozkan, E., and Kelkar, M., 2005, "Effects of Formation Damage and High-Velocity Flow on the Productivity of Perforated Horizontal Wells," SPE Reservoir Eval. Eng., **8**(4), pp. 315–324.

[16] Harding, T. G., Norris, B., and Smith, K. H., 2002, "Horizontal Water Disposal Well Performance in a High Porosity and Permeability Reservoir," SPE International Thermal Operations and Heavy Oil Symposium and International Well Technology Conference, Calgary, Alberta, CA, Nov. 4–7, Paper No. SPE-PSCIM/CHOA-79007.

[17] Harding, T. G., Varner, J., Flexhaug, L. A., and Bennion, D. B., 2003, "Design and Performance of a Water Disposal Well Stimulation Treatment in a High Porosity and Permeability Sand," Petroleum Society's Canadian International Petroleum Conference, Calgary, Alberta, CA, Jun. 10–12.

[18] Rousseau, D., Hadi, L., and Nabzar, L., 2007, "PWRI-Induced Injectivity Decline: New Insights on In-Depth Particle Deposition Mechanisms," SPE European Formation Damage Conference, Sheveningen, The Netherlands, May 30–Jun. 1, Paper No. SPE-07666.

[19] Wennberg, K. E., and Sharma, M. M., 1997, "Determination of the Filtration Coefficient and the Transition Time for Water Injection Wells," SPE European Formation Damage Conference, The Hague, The Netherlands, Jun. 2–3, Paper No. SPE-38181.

[20] Nabzar, L., Chauveteau, G., and Roque, C., 1996, "A New Model for Formation Damage by Particle Retention," SPE Formation Damage Control Conference, Lafayette, LA, Feb. 14–15, Paper No. SPE-311190.

[21] Chauveteau, N. L., and Coste, J.-P., 1998, "Physics and Modelling of Permeability Damage Induced by Particle Deposition," SPE Formation Damage Control Conference, Lafayette, LA, Feb. 18–19, Paper No. SPE-39463.

[22] Wang, S., and Civan, F., 2005, "Modeling Formation Damage by Asphaltene Deposition During Primary Oil Recovery," ASME J. Energy Resour. Technol., **127**(4), pp. 310–317.

[23] Tiab, D., and Donaldson, E. C., 1996, *Petrophysics—Theory and Practice of Measuring Reservoir Rock and Fluid Transport Properties*, Gulf, Houston, TX, p. 706.

[24] Al-Abduwani, F. A. H., Shirzadi, A., van den Broek, W. M. G. T., and Currie, P. K., 2005, "Formation Damage vs. Solid Particles Deposition Profile During Laboratory-Simulated Produced-Water Reinjection," SPEJ, **10**(2), pp. 138–151.

[25] Nabzar, L., Aguilera, M. E., and Rajoub, Y., 2005, "Experimental Study on Asphaltene-Induced Formation Damage," SPE International Symposium Oilfield Chemistry, Houston, TX, Feb. 2–4, Paper No. SPE-93062.

[26] Bedrikovetsky, P. G., 1993, *Mathematical Theory of Oil and Gas Recovery*, Kluwer Academic, Dordrecht.

[27] Todd, A. C., and Scott, G., 1984, "The Application of Depth of Formation Damage Measurements in Predicting Water Injectivity Decline," Formation Damage Control Symposium, Bakersfield, CA, Feb. 13–14, Paper No. SPE-12498.

[28] Bedrikovetsky, P., 2008, "Upscaling of Stochastic Micro Model for Suspension Transport in Porous Media," Transp. Porous Media, **75**(3), pp. 335–369.

AUTHOR QUERIES — 013003JRG

#1 Au: Please supply complete postal address for Petrobras.

#2 Au: Please define DLVO if possible.